Maternal and zygotic *Zfp57* modulate NOTCH signaling in cardiac development

Yulia Shamis[a,b,1], Dana E. Cullen[a,1], Lizhi Liu[a,1], Guan Yang[c,2], Sheau-Fang Ng[a,2], Lijuan Xiao[a,2], Fong T. Bell[a], Chelsea Ray[a], Sachiko Takikawa[a], Ivan P. Moskowitz[d], Chen-Leng Cai[a], Xiao Yang[c], and Xiajun Li[a,b,e,3]

[a]Department of Developmental and Regenerative Biology, [e]Black Family Stem Cell Institute, and [b]Department of Oncological Sciences, Icahn School of Medicine at Mount Sinai, New York, NY 10029; [c]State Key Laboratory of Proteomics, Genetic Laboratory of Development and Diseases, Institute of Biotechnology, Beijing 100071, China; and [d]Departments of Pediatrics, Pathology, and Human Genetics, University of Chicago, Chicago, IL 60637

Edited by Iva Greenwald, Columbia University, New York, NY, and approved March 10, 2015 (received for review August 12, 2014)

Zfp57 **is a maternal–zygotic effect gene that maintains genomic imprinting. Here we report that *Zfp57* mutants exhibited a variety of cardiac defects including atrial septal defect (ASD), ventricular septal defect (VSD), thin myocardium, and reduced trabeculation. *Zfp57* maternal-zygotic mutant embryos displayed more severe phenotypes with higher penetrance than the zygotic ones. Cardiac progenitor cells exhibited proliferation and differentiation defects in *Zfp57* mutants. ZFP57 is a master regulator of genomic imprinting, so the DNA methylation imprint was lost in embryonic heart without ZFP57. Interestingly, the presence of imprinted DLK1, a target of ZFP57, correlated with NOTCH1 activation in cardiac cells. These results suggest that ZFP57 may modulate NOTCH signaling during cardiac development. Indeed, loss of ZFP57 caused loss of NOTCH1 activation in embryonic heart with more severe loss observed in the maternal-zygotic mutant. Maternal and zygotic functions of *Zfp57* appear to play redundant roles in NOTCH1 activation and cardiomyocyte differentiation. This serves as an example of a maternal effect that can influence mammalian organ development. It also links genomic imprinting to NOTCH signaling and particular developmental functions.**

ZFP57 | NOTCH | cardiac development | genomic imprinting | maternal-zygotic mutant

Approximately 0.8% of live births carry congenital heart defects (CHDs) (1). Nearly 30% of lost pregnancies may have cardiac malformations (2–4). Cardiac septation defects are among the most common CHDs (2). Certain transcription factors including NKX2.5, GATA4, and TBX5 are required for cardiac septation (2).

LIN-12/NOTCH signaling is an important pathway in cell-fate specification (5–7). It is conserved in metazoa from *Caenorhabditis elegans* to humans (8). During cardiac development, it is essential for cardiomyocyte differentiation, valve development, ventricular trabeculation, and outflow tract development (9–11). It is reported that *Nkx2.5* is a direct downstream target gene of NOTCH signaling in cardiac development (12).

Zfp57 is the first identified mammalian maternal-zygotic effect gene (13). Loss of zygotic *Zfp57* causes partial neonatal lethality, whereas eliminating both maternal and zygotic *Zfp57* results in highly penetrant embryonic lethality around midgestation (13). ZFP57 is a master regulator of many imprinted genes characterized by parental origin-dependent expression (14–16). Many imprinted genes are clustered and coregulated by a *cis*-acting imprinting control region (ICR) (14). ZFP57 maintains the DNA methylation imprint at ICRs (13, 17). The imprint is partially lost in the *Zfp57* zygotic mutant but absent in the maternal-zygotic mutant (13). Expression of the imprinted genes is deregulated without ZFP57 (13).

Based on the literature, we hypothesized that the midgestational embryonic lethality present in the *Zfp57* maternal-zygotic mutant may result from abnormalities in cardiac development (18). Indeed, *Zfp57* mutants exhibited atrial septal defects (ASDs), ventricular septal defects (VSDs), thin myocardium, and reduced trabeculation, with more penetrant and worse phenotypes present in the maternal-zygotic mutant. We found NOTCH signaling was attenuated in the heart of *Zfp57* mutant embryos, which may underlie these cardiac defects.

Results

Multiple Cardiac Defects Were Observed in the *Zfp57* Mutant. *Zfp57* has both maternal (M) and zygotic (Z) functions (13) (*SI Appendix*, Fig. S1). Loss of just zygotic function of *Zfp57* (M^+Z^-) causes partial neonatal lethality, whereas elimination of both maternal and zygotic functions of *Zfp57* (M^-Z^-) results in highly penetrant maternal-zygotic embryonic lethality around midgestation (13) (*SI Appendix*, Fig. S1). *Zfp57* maternal-zygotic mutant, $^{-/-}mz$ (M^-Z^-), embryos begin dying at embryonic day 11.5 (E11.5) (13). Because lethality around midgestation can be associated with cardiac defects, we examined the hearts of $^{-/-}mz$ (M^-Z^-) embryos derived from the timed matings between *Zfp57* homozygous ($^{-/-}$) female mice and *Zfp57* heterozygous ($^{+/-}$) male mice or the hearts of *Zfp57* zygotic mutant, $^{-/-}z$ (M^+Z^-), embryos obtained from the matings between *Zfp57* heterozygous ($^{+/-}$) female mice and *Zfp57* homozygous ($^{-/-}$) male mice (*SI Appendix*, Fig. S1). As illustrated below, we found that *Zfp57* mutants, $^{-/-}mz$ (M^-Z^-) and $^{-/-}z$ (M^+Z^-), exhibited ASDs, VSDs, thin myocardium, and trabeculation defects, with higher penetrance and worse defects present in the $^{-/-}mz$ (M^-Z^-) than in the $^{-/-}z$ (M^+Z^-) hearts (Fig. 1).

ASD. Mouse cardiac septation occurs between E11.5 and E14.5 (2). The hearts of live E14.5 embryos were subjected to serial

Significance

Abnormal heart development is a common birth defect. Genomic imprinting is absolutely essential for mammalian embryonic development. We found that loss of ZFP57, a master regulator of genomic imprinting, causes a number of heart morphogenetic defects. These cardiac defects are reminiscent of mutant phenotypes observed in the NOTCH signaling pathway, one of the most important pathways in development. Indeed, we demonstrate that NOTCH signaling is diminished without ZFP57. Furthermore, the maternal function of *Zfp57* contributes to NOTCH signaling and embryonic heart development. Maternal and zygotic *Zfp57* play redundant roles in genomic imprinting, NOTCH signaling, and heart development. Thus, our results provide mechanistic links among maternal effect, genomic imprinting, NOTCH signaling, and cardiac development.

Author contributions: X.L. designed research; Y.S., D.E.C., L.L., G.Y., S.F.N., L.X., F.T.B., C.R., S.T., and I.P.M. performed research; C.L.C. and X.Y. contributed new reagents/analytic tools; Y.S., D.E.C., L.L., and X.L. analyzed data; and Y.S., D.E.C., and X.L. wrote the paper.

The authors declare no conflict of interest.

This article is a PNAS Direct Submission.

[1]Y.S., D.E.C., and L.L. contributed equally to this work.

[2]G.Y., S.F.N., and L.X. contributed equally to this work.

[3]To whom correspondence should be addressed. Email: Xiajun.Li@mssm.edu.

This article contains supporting information online at www.pnas.org/lookup/suppl/doi:10.1073/pnas.1415541112/-/DCSupplemental.

sectioning followed by hematoxalin and eosin (H&E) staining, with the whole-heart and section heart images of $^{-/+}$ (M^-Z^+) and $^{-/-}mz$ (M^-Z^-) embryos shown here (Fig. 1*A* and *SI Appendix*, Fig. S2 *A* and *B*). All ($n = 14$) live $^{-/-}mz$ (M^-Z^-) E14.5 embryos displayed secundum ASD, whereas none of the live $^{+/-}$ (M^+Z^+) ($n = 7$) or $^{-/+}$ (M^-Z^+) ($n = 13$) E14.5 embryos had ASD (Fig. 1 *A* and *B*). About 44% ($n = 9$) of the live $^{-/-}z$ (M^+Z^-) E14.5 embryos also exhibited ASD (Fig. 1*B*).

Zfp57 zygotic mutants, $^{-/-}z$ (M^+Z^-), displayed partial neonatal lethality with 40% death by postnatal day 1 (P1) (13). Indeed, most (>80%, $n = 14$) dead $^{-/-}z$ (M^+Z^-) neonatal (P0–P2) pups had ASD, whereas no ASD was observed in the hearts of live $^{-/-}z$ (M^+Z^-) ($n = 5$) or live $^{+/-}$ (M^+Z^+) ($n = 5$) neonatal pups (Fig. 1 *F* and *G* and *SI Appendix*, Fig. S2 *C–E*). We also examined the hearts of E18.5 embryos. About 40% ($n = 19$) of live $^{-/-}z$ (M^+Z^-) E18.5 embryos displayed secundum ASDs, whereas none ($n = 12$) of the $^{+/-}$ (M^+Z^+) E18.5 embryos exhibited ASD (*SI Appendix*, Fig. S2 *F–H*).

VSD. In addition to ASDs, we observed VSDs in 80% ($n = 13$) of live $^{-/-}mz$ (M^-Z^-) E14.5 embryos. Although none of the live $^{-/+}$ (M^-Z^+) E14.5 embryos had ASD (Fig. 1*B*), 20% ($n = 15$) of $^{-/+}$ (M^-Z^+) E14.5 embryos lacking maternal *Zfp57* exhibited VSDs (Fig. 1*C*). VSDs were also observed in 20% ($n = 10$) of live $^{-/-}z$ (M^+Z^-) E14.5 embryos, but not in live $^{+/-}$ (M^+Z^+) E14.5 embryos (0%, $n = 10$) derived from heterozygous female mice (Fig. 1*C*). VSD was not observed in live $^{+/-}$ (M^+Z^+) ($n = 5$) or live $^{-/-}z$ (M^+Z^-) ($n = 5$) neonatal P2 pups (Fig. 1*H*). About 20% ($n = 14$) of dead $^{-/-}z$ (M^+Z^-) P2 pups had VSDs (Fig. 1*H*).

Thin myocardium. The ventricular myocardium (vm) of $^{-/-}z$ (M^+Z^-) E14.5 embryos was significantly thinner than that of $^{+/-}$ (M^+Z^+) E14.5 embryos (Fig. 1*D*). $^{-/-}mz$ (M^-Z^-) E14.5 embryos also had a thinner vm than $^{-/+}$ (M^-Z^+) or $^{+/-}$ (M^+Z^+) E14.5 embryos (Fig. 1 *A* and *D*). The vm of $^{-/-}mz$ (M^-Z^-) E14.5 embryos appeared to be thinner than that of $^{-/-}z$ (M^+Z^-) E14.5 embryos although the difference was not statistically significant (Fig. 1*D*). Interestingly, $^{-/-}z$ (M^+Z^-) and $^{-/+}$ (M^-Z^+) E14.5 embryos had similar vm, and they both had a thinner vm than $^{+/-}$ (M^+Z^+) E14.5 embryos (Fig. 1*D*). Thus, loss of either maternal or zygotic *Zfp57* (M^- or Z^-) causes reduced vm. This implies that both maternal and zygotic *Zfp57* contribute to the normal development of ventricular myocardium and they have partially redundant roles.

Trabeculation defect. Mouse cardiac trabeculation begins at E9.5 shortly after cardiac looping occurs (19). We examined and measured the trabeculae (trab) of E14.5 embryos (Fig. 1 *A* and *E*). $^{-/-}z$ (M^+Z^-) and $^{-/-}mz$ (M^-Z^-) E14.5 embryos had similar trab that was diminished compared with $^{+/-}$ (M^+Z^+) E14.5 embryos (Fig. 1*E*). $^{-/+}$ (M^-Z^+) E14.5 embryos also appeared to have reduced trab compared with $^{+/-}$ (M^+Z^+) E14.5 embryos although the difference was not statistically significant (Fig. 1*E*). There was no significant difference in trab between $^{-/+}$ (M^-Z^+) embryos lacking maternal *Zfp57*, $^{-/-}z$ (M^+Z^-) embryos lacking zygotic *Zfp57*, and $^{-/-}mz$ (M^-Z^-) embryos lacking both maternal and zygotic *Zfp57*. This finding indicates that zygotic *Zfp57* is required for ventricular trabeculation and maternal *Zfp57* does not appear to be redundant with zygotic *Zfp57* in this process (Fig. 1*E*).

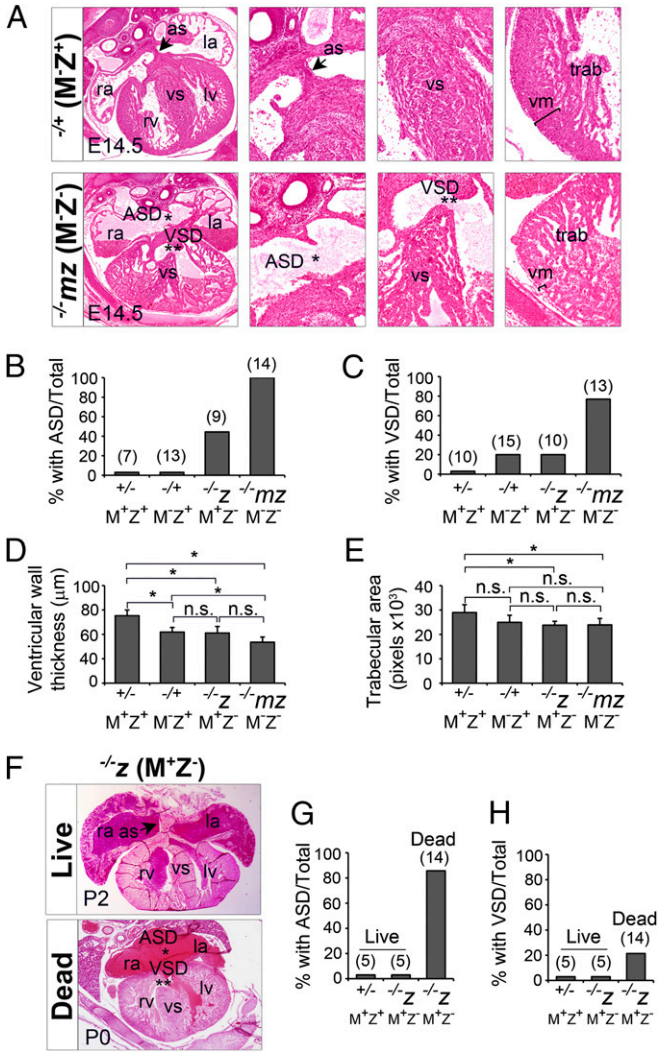

Fig. 1. Loss of ZFP57 causes multiple cardiac defects in mouse embryos and neonatal pups. The *Zfp57*$^{-/+}$ (M^-Z^+) and $^{-/-}mz$ (M^-Z^-) samples were generated from the crosses between homozygous ($^{-/-}$) female mice and heterozygous ($^{+/-}$) male mice. The $^{+/-}$ (M^+Z^+) and $^{-/-}z$ (M^+Z^-) samples were generated from the heterozygous intercrosses. ra, right atrium; rv, right ventricle; la, left atrium; lv, left ventricle; as, atrial septum (arrow); ASD, atrial septal defect (*); vs, ventricular septum; VSD, ventricular septal defect (**); vm, ventricular myocardial wall (bracket); trab, trabeculae. (*A*) H&E-stained transverse sections through the heart of *Zfp57* $^{-/+}$ and $^{-/-}mz$ E14.5 embryos with an image of 5× object lens (*Left*) and the images of 20× object lens for the enlarged area of as or ASD, vs or VSD, vm and trab, respectively. (*B* and *C*) Percentage (%) of the embryos with ASD (*B*) or VSD (*C*). The number above each bar indicates the number of embryos analyzed for each genotype. (*D* and *E*) Average ventricular wall (vm) thickness (*D*) or trabecular area (*E*). ImageJ software was used to measure multiple areas of the heart sections for each sample. Values are mean ± SEM. ANOVA was performed for statistical comparisons, followed by the post hoc independent sample *t* test with Bonferroni correction. *$P < 0.05$. n.s., statistically not significant. (*F*) Images (5× object lens) of live (*Top*) or dead (*Bottom*) neonatal (P0–P2) zygotic mutant, $^{-/-}z$ (M^+Z^-), pups. (*G* and *H*) Percentage of neonatal live or dead pups with ASD (*G*) or VSD (*H*). The number above each bar indicates the number of pups analyzed for each group.

Expression of *Zfp57* in the Heart. We used alkaline phosphatase-conjugated digoxigenin (DIG)-labeled RNA probes to detect expression of *Zfp57* in wild-type E10.5 and E13.5 embryos by RNA in situ hybridization (Fig. 2*A* and *SI Appendix*, Fig. S3). *Zfp57* was highly expressed in the spine (neural tube in *SI Appendix*, Fig. S3*A* and central canal in *SI Appendix*, Fig. S3*B*) and lung (lu in *SI Appendix*, Fig. S3*B*). *Zfp57* was also clearly expressed in the heart, although not as highly as in the spine or lung (Fig. 2 *A* and *H* and *SI Appendix*, Fig. S3). *Zfp57*-expressing cells were broadly but not uniformly distributed in the four heart chambers of wild-type, $^{+/+}$ (M^+Z^+), E10.5 embryos (*SI Appendix*, Fig. S3*C*). Notable expression of *Zfp57* was observed in the atrial septum (as), cushion tissue (ct), vm, and epicardium of wild-type, $^{+/+}$ (M^+Z^+), E13.5 embryos (Fig. 2*A*). Some spotty expression was also detected in the ventricular septum (vs) and endocardium (*SI Appendix*, Fig. S3 *C* and *D*). Consistent with the presence of a weak aberrant transcript in *Zfp57* mutant embryos carrying two deleted alleles of *Zfp57* based on Northern blot (13), a much reduced signal was detected in $^{-/-}mz$ (M^-Z^-) E13.5

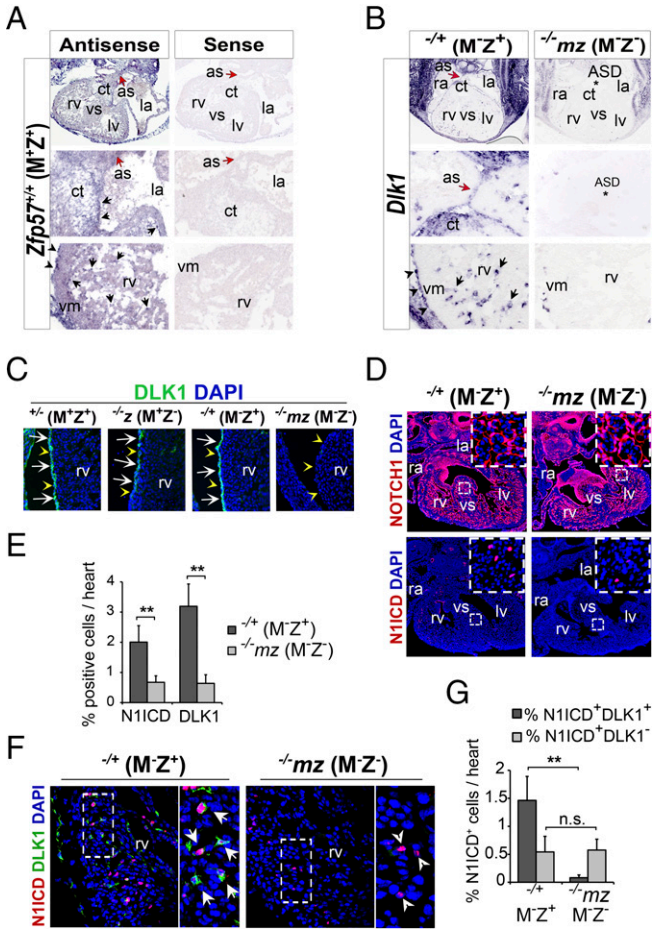

Fig. 2. *Dlk1* expression and NOTCH1 activation were both inhibited in the heart without ZFP57. The embryonic heart sections were subjected to RNA in situ hybridization (*A* and *B*) or immunostaining (*C*–*G*). Wild-type, $^{+/+}$ (M^+Z^+), E13.5 embryos in *A* were derived from the cross between wild-type female mice and wild-type male mice. $^{-/-}mz$ (M^-Z^-) and $^{-/+}$ (M^-Z^+) E13.5 embryos in *B*–*G* were derived from the cross between *Zfp57* homozygous ($^{-/-}$) female mice and heterozygous ($^{+/-}$) male mice, whereas $^{+/-}$ (M^+Z^+) and $^{-/-}z$ (M^+Z^-) E13.5 embryos in *C* were generated from the timed mating between *Zfp57*$^{+/-}$ female mice and *Zfp57* $^{-/-}$ or $^{+/-}$ male mice. ra, right atrium; rv, right ventricle; la, left atrium; lv, left ventricle; as, atrial septum; ct, cushion tissue; ASD, atrial septal defect (*); vs, ventricular septum; vm, ventricular myocardium. Blue signal in *C*, *D*, and *F*, DAPI staining. ImageJ software was used to count N1ICD-positive (N1ICD$^+$) or DLK1-positive (DLK1$^+$) cells. Standard Student's *t* test was used to analyze datasets for $^{-/-}mz$ (M^-Z^-) (gray bar) and $^{-/+}$ (M^-Z^+) (black bar) E13.5 embryos. Values are mean ± SEM, Student's *t* test: $^{**}P < 0.01$. n.s., statistically not significant. (*A*) Section RNA in situ hybridization (purple blue) with the antisense probe (*Left*) or sense probe (*Right*) of *Zfp57* transcribed from a plasmid containing the full-length *Zfp57* cDNA of 1.35 kb (13). Red arrow, atrial septum (as). Arrow, purple blue dots indicating *Zfp57*-positive cells. Arrowhead, epicardium. (*B*) Section RNA in situ hybridization (purple blue) with antisense probe of *Dlk1*. Red arrow, atrial septum (as). Asterisk (*), atrial septal defect (ASD). Arrow, purple blue dots indicating *Dlk1*-positive cells. Arrowhead, epicardium. (*C*) Immunostaining of DLK1 (green) on cryosections. Blue signal, DAPI staining. White arrow, cell surface staining of DLK1 surrounding blue nuclei. Yellow arrowhead, epicardium of the right ventricle (rv). (*D*) Immunostaining (red) of full-length NOTCH1 (*Top*) and cleaved NOTCH1 (N1ICD, *Bottom*) on paraffin-embedded sections. The *Inset* images represent the boxed areas in white dotted lines in each panel with a higher magnification (40×). (*E*) Percentage (%) of N1ICD-positive (N1ICD$^+$) or DLK1-positive (DLK1$^+$) cells in the heart relative to the total number of DAPI-positive cells in $^{-/-}mz$ (M^-Z^-) or $^{-/+}$ (M^-Z^+) E13.5 embryos. (*F*) Coimmunostaining of DLK1 (green) and N1ICD (red) on cryosections. The boxed area of rv in white dotted lines is shown on the *Right* as an enlarged image for the coimmunostained heart section. White arrows, red-stained nuclei inside green-colored cell surface, i.e., N1ICD$^+$DLK1$^+$ cells. White arrowheads, red-stained nuclei without green-colored cell surface, i.e., N1ICD$^+$DLK1$^-$ cells. (*G*) Percentage (%) of N1ICD$^+$DLK1$^+$ (double positive for N1ICD and DLK1) or N1ICD$^+$DLK1$^-$ (N1ICD-positive but DLK1-negative) cells in the heart relative to the total number of DAPI-positive cells in either $^{-/-}mz$ (M^-Z^-) or $^{-/+}$ (M^-Z^+) E13.5 embryos.

embryos including the spine, lung, and heart regions (*SI Appendix*, Fig. S3*E*). These results suggest that *Zfp57* is expressed in the embryonic heart including the corresponding regions where the aforementioned cardiac defects were observed in *Zfp57* mutants.

Genomic Imprinting Was Lost in the Heart of *Zfp57* Mutants. Previously, we found that ZFP57 maintains the DNA methylation imprint in mouse embryos (13). To examine if genomic imprinting was lost in the heart without ZFP57, we performed combined bisulphite restriction analysis (COBRA) of genomic DNA samples from the hearts of *Zfp57* $^{-/-}mz$ (M^-Z^-) E13.5 embryos and littermate $^{-/+}$ (M^-Z^+) embryos. Indeed, the DNA methylation imprint was lost in the embryonic heart at the intergenic germline-derived differentially methylated region (IG-DMR) of the *Dlk1-Dio3* imprinted region as well as at the *Peg1*, *Peg3*, and *Peg5* but not *H19* imprinted regions (*SI Appendix*, Fig. S4*A*).

NOTCH Signaling Pathway Was Perturbed in the Heart of *Zfp57* Mutants. The imprinted *Dlk1* gene at the *Dlk1-Dio3* imprinted domain encodes a protein that shares homology with classical ligands for NOTCH receptors (20–23). However, DLK1 lacks the Delta/Serrate/LAG-2 (DSL) domain present in all canonical DSL family of ligands for NOTCH receptors (8, 24). It was reported that OSM-11, a *C. elegans* homolog of DLK1, facilitates LIN-12/NOTCH signaling (24, 25). However, it is controversial whether it is a positive or negative regulator of NOTCH signaling in mammals (25–27).

It was previously reported that the DNA methylation imprint at the IG-DMR of the *Dlk1-Dio3* imprinted region was required for proper expression of the imprinted *Dlk1* gene (22). Similarly, we found that DNA methylation imprint at the IG-DMR of the *Dlk1-Dio3* imprinted region was lost and expression of the imprinted *Dlk1* gene was decreased in *Zfp57* mutant embryos (13). Those studies prompted us to investigate whether NOTCH signaling may be perturbed in the heart without ZFP57.

***Dlk1* expression in the heart.** Based on RNA in situ hybridization, *Dlk1* was highly expressed in the epicardium of $^{-/+}$ (M^-Z^+) E13.5 embryos, with some spotty *Dlk1*$^+$ cells in the myocardium (Fig. 2*B*). By contrast, its expression was dramatically reduced at the epicardium and myocardium of $^{-/-}mz$ (M^-Z^-) E13.5 embryos (Fig. 2*B*). *Dlk1* was expressed in the as and vm of *Zfp57* $^{-/+}$ (M^-Z^+) embryos but not in the as and vm of $^{-/-}mz$ (M^-Z^-) embryos (Fig. 2*B*). The expression pattern of *Dlk1* resembles that of *Zfp57* in the embryonic heart (Fig. 2 *A* and *B*). We obtained similar results with DLK1 immunostaining (Fig. 2*C* and *SI Appendix*, Fig. S4*B*). Indeed, DLK1 was similarly expressed at the epicardium of *Zfp57* $^{+/-}$ (M^+Z^+) and $^{-/+}$ (M^-Z^+) E13.5 embryos (Fig. 2*C*). It was partially reduced at the epicardium in $^{-/-}z$ (M^+Z^-) but almost completely missing in $^{-/-}mz$ (M^-Z^-) E13.5 embryos (Fig. 2*C*). DLK1 was also reduced in the myocardium of $^{-/-}mz$ (M^-Z^-) E13.5 embryos in comparison with $^{-/+}$ (M^-Z^+) E13.5 embryos in the repeat experiments (see the enlarged *Inset* images of *SI Appendix*, Fig. S4*B*). Loss of just zygotic *Zfp57* led to partial loss of *Dlk1* expression in the heart of $^{-/-}z$ (M^+Z^-) embryos, whereas *Dlk1* expression was not impaired in the $^{-/+}$ (M^-Z^+) embryos. By contrast, elimination of both maternal and zygotic *Zfp57* resulted in almost complete loss of *Dlk1* expression in the heart of $^{-/-}mz$ (M^-Z^-) embryos. These results suggest that maternal *Zfp57* and zygotic *Zfp57* are partially redundant in the expression of *Dlk1* in the embryonic heart.

Activation of NOTCH1 was inhibited. NOTCH1 is the predominant member of NOTCH receptors expressed in the embryonic heart (12). We used a monoclonal antibody against full-length NOTCH1 to examine its expression. We found NOTCH1 was similarly

expressed in the endocardium and myocardium of $Zfp57^{+/-}$ (M^+Z^+), $^{-/+}$ (M^-Z^+), and $^{-/-}mz$ (M^-Z^-) E13.5 embryos (Fig. 2*D* and *SI Appendix*, Fig. S4*C*).

A key activation event in NOTCH signaling is ligand-dependent γ-secretase–mediated cleavage of NOTCH receptors (5, 6, 11, 28–30). We performed immunostaining with a monoclonal antibody that can only detect the cleaved activated form of NOTCH1 receptor (N1ICD). Interestingly, we saw a marked decrease of N1ICD in the heart of $^{-/-}mz$ (M^-Z^-) E13.5 embryos compared with $Zfp57^{+/-}$ (M^+Z^+), $^{-/+}$ (M^-Z^+), or $^{-/-}z$ (M^+Z^-) E13.5 embryos (*SI Appendix*, Fig. S4*D*). N1ICD was not much reduced in the heart of $^{-/-}z$ (M^+Z^-) E13.5 embryos in comparison with $^{+/-}$ (M^+Z^+) or $^{-/+}$ (M^-Z^+) embryos (*SI Appendix*, Fig. S4*D*). N1ICD reduction in the embryonic heart without ZFP57 was confirmed in the repeat experiments comparing $^{-/-}mz$ (M^-Z^-) E13.5 embryos with $^{-/+}$ (M^-Z^+) E13.5 embryos (Fig. 2*D*). Upon quantification, we found both DLK1-positive ($DLK1^+$) cells and N1ICD-positive ($N1ICD^+$) cells decreased dramatically in the heart of $^{-/-}mz$ (M^-Z^-) embryos compared with $^{-/+}$ (M^-Z^+) embryos (Fig. 2*E*).

As expected, NOTCH1 was primarily localized on the cell surface in the heart of $^{+/-}$ (M^+Z^+), $^{-/+}$ (M^-Z^+), or $^{-/-}mz$ (M^-Z^-) E13.5 embryos (Fig. 2*D* and *SI Appendix*, Fig. S4*C*). DLK1 was also present at the cell surface in the heart of $^{+/-}$ (M^+Z^+), $^{-/+}$ (M^-Z^+), or $^{-/-}z$ (M^+Z^-) E13.5 embryos (Fig. 2*C*). To test how DLK1 may be involved in NOTCH1 activation, we performed coimmunostaining with monoclonal antibodies against DLK1 and full-length NOTCH1 in the heart. Interestingly, DLK1 was present at the cell surface of a subset of NOTCH1-positive cells in the heart of $^{-/+}$ (M^-Z^+) E13.5 embryos, but not in $^{-/-}mz$ (M^-Z^-) E13.5 embryos (*SI Appendix*, Fig. S4*E*).

We also performed coimmunostaining of DLK1 and N1ICD (Fig. 2*F*). N1ICD was predominantly localized to the nucleus in the heart of $Zfp57^{-/+}$ E13.5 embryos, whereas DLK1 was concentrated on the cell surface (Fig. 2*F*). Interestingly, most $N1ICD^+$ cells also expressed DLK1, i.e., $N1ICD^+DLK1^+$ cells (Fig. 2*F*). Although little DLK1 was expressed, nuclear N1ICD was present in a few sparsely populated cells in the heart of $^{-/-}mz$ (M^-Z^-) E13.5 embryos (Fig. 2*F*). These are $N1ICD^+DLK1^-$ cells that possibly resulted from NOTCH1 activation via DLK1-independent pathways. We quantified $N1ICD^+DLK1^+$ and $N1ICD^+DLK1^-$ cells in the heart of $^{-/-}mz$ (M^-Z^-) and $Zfp57^{-/+}$ (M^-Z^+) embryos (Fig. 2*G*). $N1ICD^+DLK1^+$ cells accounted for about 1.5% of cells in the heart of $Zfp57^{-/+}$ (M^-Z^+) embryos but were absent in the heart of $^{-/-}mz$ (M^-Z^-) embryos (Fig. 2*G*). By contrast, the number of $N1ICD^+DLK1^-$ cells remained constant, accounting for about 0.5% of cells in the heart of either $^{-/-}mz$ (M^-Z^-) or $^{-/+}$ (M^-Z^+) embryos (Fig. 2*G*). These results suggest that most N1ICD generation in the heart may be dependent on DLK1.

NOTCH1 Target Genes Were Inhibited in the Heart of *Zfp57* Mutants. *Hey1* and *Hey2* are two direct target genes of NOTCH signaling in the cardiovascular system (31). *Hey1* knockout mice do not show any obvious phenotype (31). By contrast, the *Hey2* knockout mouse exhibits ASD, VSD, and thin myocardium, similar to the *Zfp57* knockout mouse (31–34). We performed RNA in situ hybridization to examine the expression of *Hey1* and *Hey2* in the heart of E10.5 (*SI Appendix*, Fig. S5 *A* and *B*) and E13.5 (Fig. 3*A* and *SI Appendix*, Fig. S6 *A* and *B*) embryos. *Hey1* was similarly expressed in the heart of $^{-/-}mz$ (M^-Z^-) and $^{-/+}$ (M^-Z^+) E10.5 embryos (*SI Appendix*, Fig. S5*A*). Expression of *Hey1* was also similar in the heart of $Zfp57^{+/-}$ (M^+Z^+), $^{-/-}z$ (M^+Z^-), $^{-/+}$ (M^-Z^+), and $^{-/-}mz$ (M^-Z^-) embryos at E13.5, as is more clearly seen with the magnified right ventricle (rv) of these E13.5 embryos (Fig. 3*A*). This was the same in the repeat RNA in situ experiments comparing $^{-/+}$ (M^-Z^+) with $^{-/-}mz$ (M^-Z^-) E13.5 embryos, as is exemplified by the magnified rv (*SI Appendix*, Fig. S6 *A* and *B*). By contrast, *Hey2* expression was slightly reduced in the heart of $^{-/-}mz$ (M^-Z^-) E10.5 embryos compared with $^{+/-}$ (M^+Z^+) or $^{-/+}$ (M^-Z^+) E10.5 embryos, whereas it was not diminished in the heart of $^{-/-}z$ (M^+Z^-) E10.5 embryos compared with $^{+/-}$ (M^+Z^+) E10.5 embryos (*SI Appendix*, Fig. S5 *A* and *B*). *Hey2* was more profoundly down-regulated in the heart of $^{-/-}mz$ (M^-Z^-) E13.5 embryos, with the magnified image of rv as an example, although it was still similarly expressed in the heart of $^{-/+}$ (M^-Z^+), $^{+/-}$ (M^+Z^+), and $^{-/-}z$ (M^+Z^-) E13.5 embryos (Fig. 3*A*). Down-regulation of *Hey2* in $^{-/-}mz$ (M^-Z^-) E13.5 embryos versus $^{-/+}$ (M^-Z^+) E13.5 embryos was verified in the repeat RNA in situ experiments, which is more obvious with the magnified image of left ventricle (lv) (*SI Appendix*, Fig. S6 *A* and *B*). Thus, loss of just maternal or just zygotic *Zfp57* did not cause significant reduction of *Hey2*, whereas elimination of both maternal and zygotic *Zfp57* resulted in reduced expression of *Hey2* in the heart of E10.5 and E13.5 embryos. These results suggest that maternal and zygotic *Zfp57* functions play a redundant role in *Hey2* expression in the embryonic heart.

Nkx2.5 encodes a homeodomain transcription factor essential for cardiac development (35). It is a direct target gene of NOTCH1 (12). Nuclear N1ICD can activate *Nkx2.5* expression in cardiac progenitor cells (CPCs), driving CPCs to become cardiomyocytes (12). Mutations in human *NKX2.5* cause ASD and VSD (35). We examined its expression in the heart by RNA in situ hybridization. *Nkx2.5* was highly expressed throughout the myocardium of E10.5 and E13.5 embryos (Fig. 3*A* and *SI Appendix*, Figs. S5 and S6). *Nkx2.5* was similarly expressed in the heart of $^{+/-}$ (M^+Z^+) and $^{-/-}z$ (M^+Z^-) E10.5 embryos (*SI Appendix*, Fig. S5*B*), but it was slightly down-regulated in the heart of $^{-/-}mz$ (M^-Z^-) E10.5 embryos, compared with $^{-/+}$ (M^-Z^+), $^{+/-}$ (M^+Z^+), or $^{-/-}z$ (M^+Z^-) E10.5 embryos (*SI Appendix*, Fig. S5 *A* and *B*). Whereas *Nkx2.5* was similarly expressed in the heart of $^{-/+}$ (M^-Z^+), $^{+/-}$ (M^+Z^+), and $^{-/-}z$ (M^+Z^-) E13.5 embryos, its expression was significantly reduced in the heart of $^{-/-}mz$ (M^-Z^-) E13.5 embryos, as is easily seen with the magnified rv (Fig. 3*A*). Reduced *Nkx2.5* expression in $^{-/-}mz$ (M^-Z^-) E13.5 embryos compared with $^{-/+}$ (M^-Z^+) E13.5 embryos was verified in the repeat RNA in situ experiments, with the magnified lv as an example (*SI Appendix*, Fig. S6 *A* and *B*). Thus, maternal and zygotic *Zfp57* are also redundant in *Nkx2.5* expression in the embryonic heart.

Bmp10 is highly expressed in developing cardiac trabeculae (19). Loss of *Bmp10* results in ventricular trabeculation defect due to decreased cardiomyocyte proliferation. Ablation of NOTCH signaling causes reduced *Bmp10* expression and cardiomyocyte proliferation in the heart (36). Based on RNA in situ hybridization, there was no difference in *Bmp10* expression in the trabeculae of the $Zfp57^{-/+}$ (M^-Z^+) and $^{-/-}mz$ (M^-Z^-) E10.5 embryos (*SI Appendix*, Fig. S5*A*). Interestingly, *Bmp10* was similarly down-regulated in the trabeculae of both $^{-/-}mz$ (M^-Z^-) and $^{-/-}z$ (M^+Z^-) E13.5 embryos, in comparison with $^{-/+}$ (M^-Z^+) and $^{+/-}$ (M^+Z^+) E13.5 embryos, whereas its expression seemed to be similar in the trabeculae of the $^{-/+}$ (M^-Z^+) and $^{+/-}$ (M^+Z^+) E13.5 embryos (Fig. 3*A*). This down-regulation is more clearly visualized by the magnified rv (Fig. 3*A*). Down-regulation of *Bmp10* in the trabeculae of $^{-/-}mz$ (M^-Z^-) versus $^{-/+}$ (M^-Z^+) E13.5 embryos was verified in the repeat RNA in situ experiments, with the magnified lv as an example (*SI Appendix*, Fig. S6 *A* and *B*). These results suggest that only zygotic *Zfp57* is necessary and sufficient for proper expression of *Bmp10* in the trabeculae of the embryonic heart.

We also performed quantitative RT-PCR (qRT-PCR) analysis of the total RNA samples isolated from the hearts of E10.5 and E13.5 embryos. Indeed, *Nkx2.5*, but not *Hey1* or *Bmp10*, was significantly reduced in the heart of $^{-/-}mz$ (M^-Z^-) E10.5 embryos in comparison with $^{-/+}$ (M^-Z^+) E10.5 embryos (*SI Appendix*, Fig. S5*C*). Compared with $^{-/+}$ (M^-Z^+) E10.5 embryos, *Hey2* seemed to be also inhibited in the heart of $^{-/-}mz$ (M^-Z^-) E10.5 embryos (*SI Appendix*, Fig. S5*C*). Similarly, *Nkx2.5* and *Hey2* but not *Hey1* were down-regulated in the heart of $^{-/-}mz$ (M^-Z^-) E13.5 embryos compared with $^{-/+}$ (M^-Z^+) or $^{+/-}$ (M^+Z^+) or $^{-/-}z$ (M^+Z^-) E13.5 embryos (Fig. 3*B* and *SI Appendix*, Fig. S6*C*). By contrast, no down-regulation of *Nkx2.5* or *Hey2* or *Hey1*

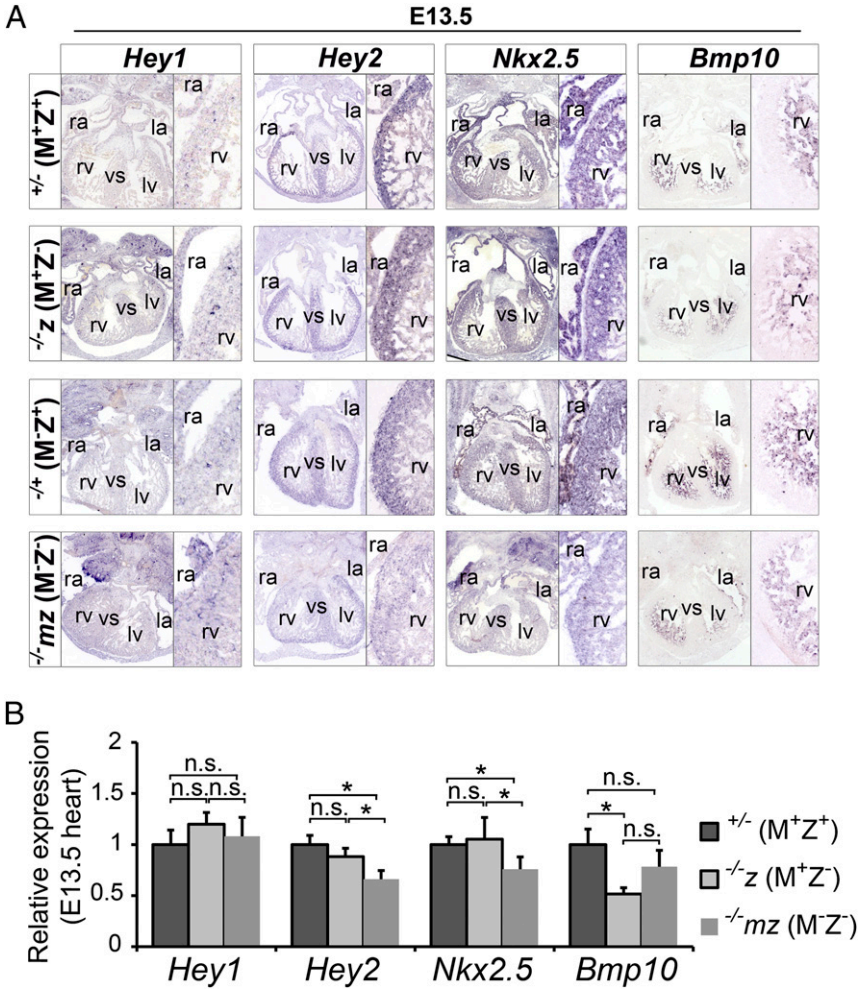

Fig. 3. Some target genes of NOTCH signaling were down-regulated in the heart without ZFP57. (*A*) RNA in situ hybridization on the heart sections of E13.5 embryos. RNA in situ hybridization (purple blue) was performed on the heart cryosections of $^{-/-}z$ (M^+Z^-) or $^{+/-}$ (M^+Z^+) E13.5 embryos derived from heterozygous female mice and $^{-/-}mz$ (M^-Z^-) or $^{-/+}$ (M^-Z^+) E13.5 embryos derived from homozygous female mice. Digoxigenin (DIG)-labeled antisense riboprobes used for RNA in situ were derived from the cDNA constructs of *Hey1*, *Hey2*, *Nkx2.5*, and *Bmp10*. ra, right atrium; la, left atrium; rv, right ventricle; lv, left ventricle; vs, ventricular septum. A portion of the rv is also shown as a magnified image on the *Right*, next to the original image for the whole heart on the *Left*. At least two independent embryos for each genotype were used for this RNA in situ hybridization. (*B*) qRT-PCR analysis of the NOTCH1 target genes in the heart of E13.5 embryos. Total RNA samples were isolated from the hearts of live *Zfp57* $^{+/-}$ (M^+Z^+), $^{-/-}z$ (M^+Z^-), and $^{-/-}mz$ (M^-Z^-) E13.5 embryos. Black filled bars, $^{+/-}$ (M^+Z^+) embryos. Light gray bars, $^{-/-}z$ (M^+Z^-) embryos. Dark gray bars, $^{-/-}mz$ (M^-Z^-) embryos. The qRT-PCR data from three biological and three technical replicates were analyzed for each experimental group. Values are mean ± SEM. Student's *t* test: $*P < 0.05$; n.s., statistically not significant.

was observed in the heart of $^{-/-}z$ (M^+Z^-) E13.5 embryos in comparison with $^{+/-}$ (M^+Z^+) E13.5 embryos (Fig. 3*B*). These qRT-PCR results are entirely consistent with the results obtained with RNA in situ hybridization for *Hey1*, *Hey2*, and *Nkx2.5*. Therefore, we conclude that maternal and zygotic *Zfp57* are redundant for expression of *Hey2* and *Nkx2.5* in the embryonic heart.

Based on qRT-PCR, *Bmp10* appeared to be down-regulated in the heart of $^{-/-}mz$ (M^-Z^-) E13.5 embryos in comparison with $^{-/+}$ (M^-Z^+) or $^{+/-}$ (M^+Z^+) E13.5 embryos (Fig. 3*B* and *SI Appendix*, Fig. S6*C*). Interestingly, *Bmp10* was similarly down-regulated in the heart of $^{-/-}z$ (M^+Z^-) E13.5 embryos (Fig. 3*B*). These qRT-PCR results for *Bmp10* are consistent with the results obtained with RNA in situ hybridization, suggesting that zygotic *Zfp57* but not maternal *Zfp57* is necessary and sufficient for *Bmp10* expression in the embryonic heart.

Taken together, at least three NOTCH1 target genes (*Hey2*, *Nkx2.5*, and *Bmp10*) were down-regulated during cardiac development without ZFP57 based on RNA in situ hybridization and qRT-PCR analysis. Therefore, we conclude that the NOTCH1 signaling pathway is inhibited in the heart of *Zfp57* mutant embryos.

Cardiomyocyte Proliferation Was Reduced. Ablation of NOTCH signaling causes reduced BMP10 signaling and decreased cardiomyocyte proliferation (36). To determine if cardiomyocyte proliferation was reduced without ZFP57, we performed EdU incorporation assay in the heart of E13.5 embryos (Fig. 4). EdU labeling appeared to be reduced in the heart of $^{-/-}mz$ (M^-Z^-) E13.5 embryos in comparison with $^{+/-}$ (M^+Z^+), $^{-/-}z$ (M^+Z^-), or $^{-/+}$ (M^-Z^+) E13.5 embryos, whereas similar EdU labeling was observed in $^{+/-}$ (M^+Z^+) and $^{-/-}z$ (M^+Z^-) E13.5 embryos, as is exemplified by the magnified heart regions (Fig. 4 *A* and *B*). When quantified, significantly fewer EdU-positive (EdU^+) cells (one-third decrease) were observed in the heart of $^{-/-}mz$ (M^-Z^-) E13.5 embryos compared with $^{-/+}$ (M^-Z^+) embryos (Fig. 4*C*). This finding was verified with a BrdU-incorporation assay (*SI Appendix*, Fig. S7*A*). The number of $BrdU^+$ cells was reduced throughout the heart of $^{-/-}mz$ (M^-Z^-) E13.5 embryos in comparison with $^{-/+}$ (M^-Z^+) E13.5 embryos. $BrdU^+$ cells were reduced by one-third in $^{-/-}mz$ (M^-Z^-) embryos (*SI Appendix*, Fig. S7*C*), similar to what was observed with EdU labeling (Fig. 4*C*). However, the percentage of $BrdU^+$ cells in the heart of $^{-/+}$ (M^-Z^+) or $^{-/-}mz$ (M^-Z^-) E13.5 embryos was about half of the percentage of

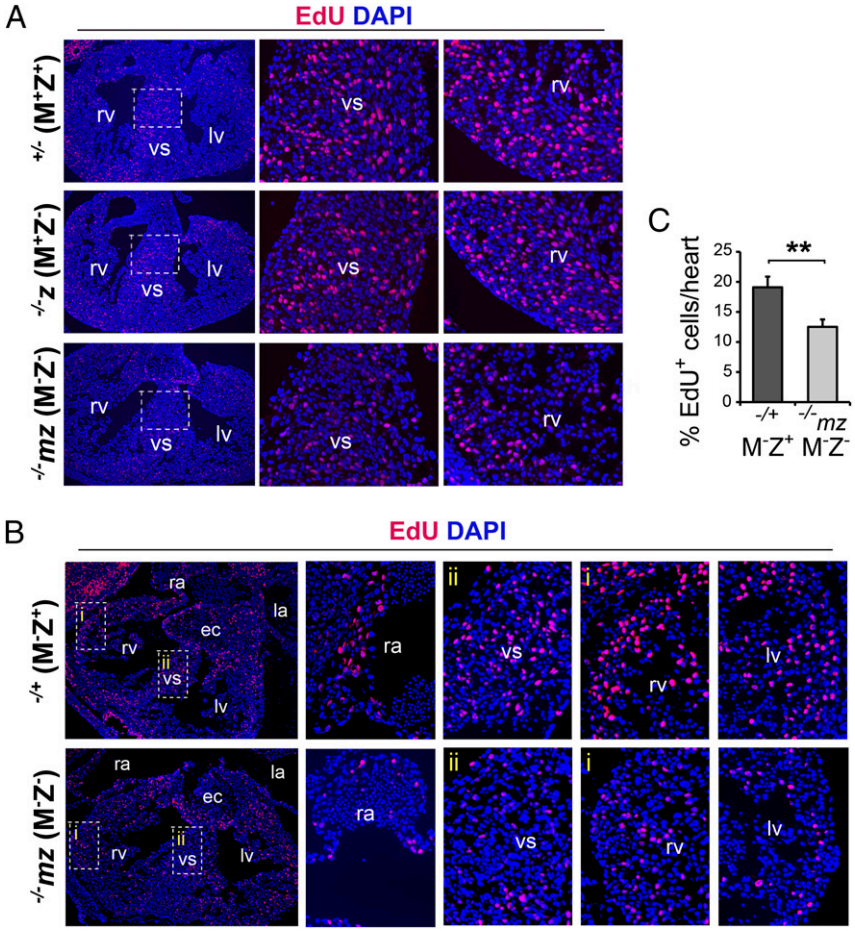

Fig. 4. Loss of ZFP57 caused reduced proliferation in the heart of E13.5 embryos. Immunostaining (red) was performed on the heart cryosections of E13.5 embryos derived from EdU-injected pregnant heterozygous or homozygous female mice. *Zfp57*$^{+/-}$ (M^+Z^+) and $^{-/-}z$ (M^+Z^-) E13.5 embryos were generated from the timed mating between *Zfp57* heterozygous female mice and homozygous or heterozygous male mice, whereas $^{-/-}mz$ (M^-Z^-) and $^{-/+}$ (M^-Z^+) E13.5 embryos were derived from the cross between *Zfp57* homozygous female mice and heterozygous male mice. Red signal, nuclei of EdU-labeled cells. Blue signal, DAPI-stained nuclei. ra, right atrium; rv, right ventricle; la, left atrium; lv, left ventricle; vs, ventricular septum; ec, endocardial cushion. (*A*) Anti-EdU immunostaining on the heart cryosections of $^{+/-}$ (M^+Z^+), $^{-/-}z$ (M^+Z^-), and $^{-/-}mz$ (M^-Z^-) E13.5 embryos. A portion of the magnified vs or rv is shown on the *Right*, next to the heart image of lower magnification. Boxes in white dotted lines show the areas of vs that are shown as the magnified images on the *Right*. (*B*) Anti-EdU immunostaining on the heart cryosections of $^{-/+}$ (M^-Z^+) and $^{-/-}mz$ (M^-Z^-) E13.5 embryos. A portion of the magnified ra, vs, rv, or lv is shown on the *Right*, next to the heart image of lower magnification. Boxes in white dotted lines show the areas of vs (*ii*) and rv (*i*) that are shown as the magnified images on the *Right*. (C) Percentage of EdU-positive (% EdU^+) cells in the heart relative to DAPI-positive cells. ImageJ software was used to quantify the numbers of immunostained cells or DAPI-stained cells. Black filled bar, *Zfp57* $^{-/+}$ (M^-Z^+) embryos. Gray filled bar, $^{-/-}mz$ (M^-Z^-) embryos. At least three independent E13.5 embryos were analyzed for each group. Values are mean ± SEM. Student's *t* test: $^{**}P < 0.01$.

EdU^+ cells in the heart of $^{-/+}$ (M^-Z^+) or $^{-/-}mz$ (M^-Z^-) E13.5 embryos, respectively. Because our BrdU labeling protocol required hydrochloride (HCl) treatment, this led to partial destruction of the nuclei that made it difficult for us to accurately quantify cell numbers and percentages of $BrdU^+$ cells. By contrast, our EdU labeling protocol was much simpler and the data obtained with EdU labeling could accurately reflect percentages of proliferating cells in the heart. Thus, most of our cell proliferation assays were done with the EdU labeling method (Figs. 4 *A* and *B* and 5 *D* and *E* and *SI Appendix*, Figs. S10 and S11). Nevertheless, the results obtained from both EdU and BrdU labeling experiments arrive at similar conclusions that the portion of the cells undergoing proliferation is reduced in the embryonic heart without ZFP57.

To examine whether apoptosis would play a role in the cardiac defects of *Zfp57* mutant embryos, we performed immunostaining with antibodies against cleaved Caspase-3. Similar Caspase-3 immunostaining was observed in the heart of $^{-/-}mz$ (M^-Z^-) and $^{-/+}$ (M^-Z^+) E13.5 embryos, as is exemplified by the magnified images of rv and vs (*SI Appendix*, Fig. S7*B*). When quantified, there was no significant difference in the number of Caspase-3-positive cells in the heart comparing $^{-/-}mz$ (M^-Z^-) with $^{-/+}$ (M^-Z^+) E13.5 embryos (*SI Appendix*, Fig. S7*D*). Thus, apoptosis is not involved in the cardiac defects observed in *Zfp57* mutant embryos.

N-Myc is involved in cardiomyocyte proliferation (37, 38). Interestingly, its expression was down-regulated in the heart of $^{-/-}z$ (M^+Z^-) E13.5 embryos in comparison with $^{+/-}$ (M^+Z^+) E13.5 embryos but not as much as in $^{-/-}mz$ (M^-Z^-) E13.5 embryos based on qRT-PCR analysis (*SI Appendix*, Fig. S8*A*). Indeed, *N-Myc* expression was significantly reduced in the heart of $^{-/-}mz$ (M^-Z^-) E13.5 embryos in comparison with $^{-/-}z$ (M^+Z^-) or $^{-/+}$ (M^-Z^+) E13.5 embryos (*SI Appendix*, Fig. S8 *A* and *B*). These results indicate that both maternal and zygotic *Zfp57* are required for full expression of *N-Myc* in the embryonic heart and their roles are not redundant in *N-Myc* expression. Inhibition of *N-Myc* may also contribute to cardiomyocyte proliferation defect in *Zfp57* mutant embryos.

Differentiation of CPCs Was Inhibited. Because NOTCH signaling is crucial for cell-fate specification, we wondered if cardiomyocyte

differentiation may be affected without ZFP57. C-KIT is a common marker for hematopoietic stem cells and progenitor cells (39, 40). It is also reported to be expressed in CPCs (12). Indeed, *c-Kit* was increased by about threefold in the heart of $^{-/-}mz$ (M^-Z^-) E10.5 embryos versus $^{-/+}$ (M^-Z^+) E10.5 embryos based on qRT-PCR analysis (*SI Appendix*, Fig. S8*C*). It was also increased in the heart of $^{-/-}mz$ (M^-Z^-) E13.5 embryos compared with $^{+/-}$ (M^+Z^+), $^{-/+}$ (M^-Z^+), or $^{-/-}z$ (M^+Z^-) E13.5 embryos based on qRT-PCR analysis, whereas there was no difference in *c-Kit* expression comparing $^{-/-}z$ (M^+Z^-) with $^{+/-}$ (M^+Z^+) E13.5 embryos (*SI Appendix*, Fig. S8 *D* and *E*). These findings were confirmed by c-KIT immunostaining. Although it was similarly expressed in the heart of $^{+/-}$ (M^+Z^+), $^{-/+}$ (M^-Z^+), and $^{-/-}z$ (M^+Z^-) E13.5 embryos, c-KIT was significantly increased in the heart of $^{-/-}mz$ (M^-Z^-) E13.5 embryos based on immunostaining (Fig. 5*A*). Increased expression of c-KIT in the heart of $^{-/-}mz$ (M^-Z^-) E13.5 embryos compared with $^{-/+}$ (M^-Z^+) E13.5 embryos was confirmed in the repeat experiment and c-KIT was indeed found to be mainly localized on the cell membrane, as is more clearly visualized in the magnified inset images as well as the magnified ra, rv, and vs (*SI Appendix*, Fig. S9 *B* and *E*). When quantified, we observed twofold increase of c-KIT-positive (c-KIT$^+$) cells in the heart of $^{-/-}mz$ (M^-Z^-) E13.5 embryos compared with $^{-/+}$ (M^-Z^+) E13.5 embryos (*SI Appendix*, Fig. S9*F*). Therefore, loss of both maternal and zygotic *Zfp57* caused significant increase of *c-Kit* expression in the embryonic heart of $^{-/-}mz$ (M^-Z^-) embryos, whereas loss of just maternal or just zygotic *Zfp57* did not result in any increased *c-Kit* expression in either $^{-/+}$ (M^-Z^+) or $^{-/-}z$ (M^+Z^-) embryos. These results demonstrate that maternal and zygotic *Zfp57* are redundant in *c-Kit* expression in the embryonic heart. Accumulation of c-KIT$^+$ cells indicates that CPC differentiation is probably inhibited without ZFP57.

NKX2.5 and GATA4 are two key transcription factors required for cardiomyocyte differentiation (12, 35, 41). Based on qRT-PCR, both *Nkx2.5* and *Gata4* transcripts were down-regulated in $^{-/-}mz$ (M^-Z^-) E13.5 embryos compared with $^{-/+}$ (M^-Z^+) E10.5 embryos, although *Nkx2.5* transcript but not *Gata4* transcript was also reduced in $^{-/-}mz$ (M^-Z^-) E10.5 embryos in comparison with $^{-/+}$ (M^-Z^+) E10.5 embryos (*SI Appendix*, Fig. S8 *C* and *D*). To test if NKX2.5 protein may be also reduced without ZFP57, we performed immunostaining with antibodies against NKX2.5 in E10.5 (*SI Appendix*, Fig. S9*A*) and E13.5 (Fig. 5*B*) embryos. In agreement with our RNA in situ results for *Nkx2.5* in E10.5 embryos (*SI Appendix*, Fig. S5*B*), NKX2.5 was reduced in immunostaining in the heart of $^{-/-}mz$ (M^-Z^-) but not $^{-/-}z$ (M^+Z^-) E10.5 embryos compared with $^{+/-}$ (M^+Z^+) E10.5 embryos (*SI Appendix*, Fig. S9*A*). NKX2.5 was also decreased in the heart of $^{-/-}mz$ (M^-Z^-) E13.5 embryos in comparison with $^{+/-}$ (M^+Z^+), $^{-/+}$ (M^-Z^+), or $^{-/-}z$ (M^+Z^-) E13.5 embryos, whereas it was similar in $^{+/-}$ (M^+Z^+), $^{-/+}$ (M^-Z^+), or $^{-/-}z$ (M^+Z^-) E13.5 embryos (Fig. 5*B*). These results are in agreement with those obtained with qRT-PCR and RNA in situ for *Nkx2.5* in E13.5 embryos (Fig. 3). Reduced NKX2.5 in the heart of $^{-/-}mz$ (M^-Z^-) versus $^{-/+}$ (M^-Z^+) E13.5 embryos was confirmed by the repeat immunostaining experiments (*SI Appendix*, Fig. S9*C*). Both the number and the mean intensity of NKX2.5$^+$ cells decreased in the heart of $^{-/-}mz$ (M^-Z^-) E13.5 embryos in comparison with $^{-/+}$ (M^-Z^+) embryos (*SI Appendix*, Fig. S9 *F* and *G*).

Similarly, GATA4 protein was also down-regulated in the heart of $^{-/-}mz$ (M^-Z^-) E13.5 embryos but not in the heart of $^{-/-}z$ (M^+Z^-) E13.5 in comparison with $^{+/-}$ (M^+Z^+) or $^{-/+}$ (M^-Z^+) E13.5 embryos (Fig. 5*C*). Down-regulation of GATA4 in the heart of $^{-/-}mz$ (M^-Z^-) E13.5 embryos versus $^{-/+}$ (M^-Z^+) E13.5 embryos was verified by the repeat immunostaining experiments (*SI Appendix*, Fig. S9*D*). Upon quantification, the number of GATA4$^+$ cells also decreased in the heart of $^{-/-}mz$ (M^-Z^-) E13.5 embryos in comparison with $^{-/+}$ (M^-Z^+) E13.5 embryos (*SI Appendix*, Fig. S9*F*).

These results suggest that differentiation of CPCs into NKX2.5$^+$ or GATA4$^+$ cells is attenuated in the heart without ZFP57. Maternal and zygotic *Zfp57* are redundant in the expression of NKX2.5 and GATA4 in the embryonic heart. In our future study, we will examine if NKX2.5$^+$ or GATA4$^+$ cells are immature committed cardiomyocytes by coimmunostaining with

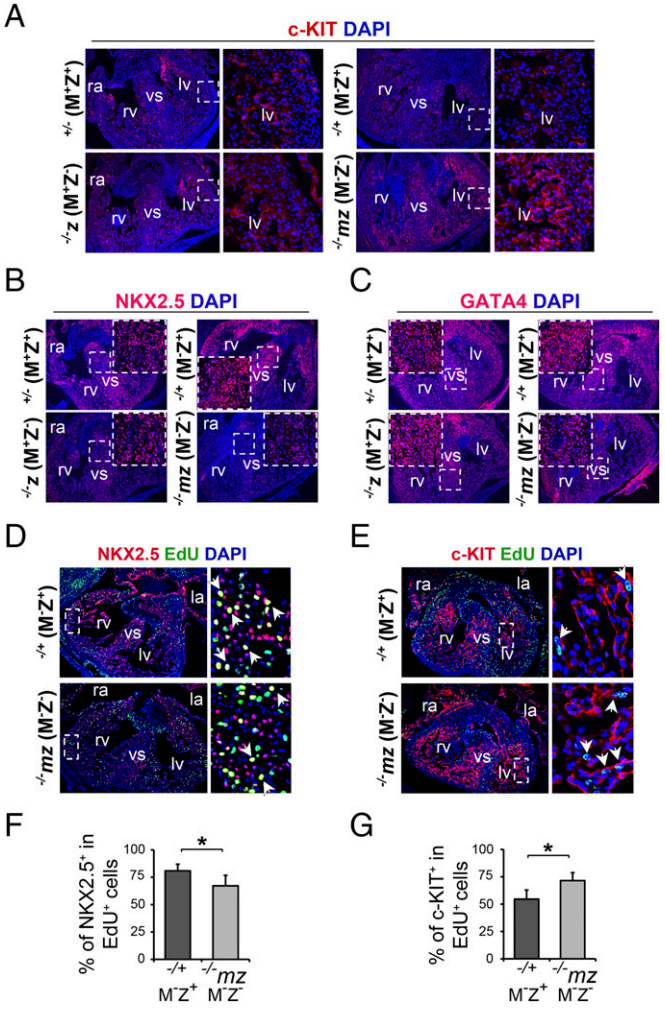

Fig. 5. Cardiac differentiation was inhibited in the heart of *Zfp57* mutant embryos. Immunostaining was performed on the heart cryosections of E13.5 embryos. *Zfp57*$^{+/-}$ (M^+Z^+) and $^{-/-}z$ (M^+Z^-) E13.5 embryos were generated from the timed mating between *Zfp57* heterozygous female mice and *Zfp57* homozygous or heterozygous male mice, whereas $^{-/-}mz$ (M^-Z^-) and $^{-/+}$ (M^-Z^+) E13.5 embryos were derived from homozygous female mice mated with heterozygous male mice. ra, right atrium; rv, right ventricle; la, left atrium; lv, left ventricle; vs, ventricular septum. Blue signal, DAPI staining. The small box in white dotted lines was magnified as an *Inset* image (the large box in white dotted lines) inside the original image of lower magnification (*B* and *C*) or as a separate image on the *Right* next to the original image of lower magnification (*A*, *D*, and *E*) in the same panel. (*A*) c-KIT immunostaining (red) of E13.5 embryos. (*B*) NKX2.5 immunostaining (red) of E13.5 embryos. (*C*) GATA4 immunostaining (red) of E13.5 embryos. (*D*) NKX2.5 (red) and EdU (green) coimmunostaining of E13.5 embryos. Arrowheads, NKX2.5 and EdU double positive (NKX2.5$^+$EdU$^+$) cells with yellow nuclei. (*E*) c-KIT (red) and EdU (green) coimmunostaining of E13.5 embryos. Arrowheads, c-KIT and EdU double positive (c-KIT$^+$EdU$^+$) cells with green nuclei inside red-colored cell surface. (*F* and *G*) ImageJ software was used to quantify the number of immunostained cells on the heart sections. Gray filled bars, $^{-/-}mz$ (M^-Z^-) E13.5 embryos. Black filled bars, $^{-/+}$ (M^-Z^+) E13.5 embryos. Values are mean ± SEM. Student's *t* test: $^*P < 0.05$. (*F*) Percentage (%) of NKX2.5$^+$ cells within the EdU$^+$ cell population in the heart, i.e., no. of NKX2.5$^+$ EdU$^+$ cells/no. of EdU$^+$ cells. (*G*) Percentage (%) of c-KIT$^+$ cells within the EdU$^+$ cell population in the heart, i.e., no. of c-KIT$^+$EdU$^+$ cells/no. of EdU$^+$ cells.

antibodies against some markers for cardiomyocytes such as contractile proteins.

Proliferating CPCs Exhibited Differentiation Defect. Overall cell proliferation was reduced in the heart of $^{-/-}mz$ (M^-Z^-) E13.5 embryos in comparison with $^{+/-}$ (M^+Z^+), $^{-/+}$ (M^-Z^+), or $^{-/-}z$ (M^+Z^-) E13.5 embryos (Fig. 4). To find out which cell types constitute the remaining proliferating cells in the heart of $^{-/-}mz$ (M^-Z^-) E13.5 embryos, we performed EdU labeling in combination with immunostaining with antibodies against NKX2.5 or c-KIT (Fig. 5 *D* and *E* and *SI Appendix*, Figs. S10 and S11). We found that the fraction of EdU^+ cells that were $NKX2.5^+$ was reduced in the heart of $^{-/-}mz$ (M^-Z^-) E13.5 embryos compared with $^{-/+}$ (M^-Z^+) E13.5 embryos (Fig. 5 *D* and *F*). By contrast, the fraction of EdU^+ cells that were c-KIT^+ was increased in the heart of $^{-/-}mz$ (M^-Z^-) E13.5 embryos versus $Zfp57^{-/+}$ (M^-Z^+) E13.5 embryos (Fig. 5 *E* and *G*). Thus, proliferating c-KIT^+ cells, i.e., presumably proliferating CPCs, accumulated, whereas proliferating $NKX2.5^+$ cells, i.e., presumably immature committed cardiomyocytes, decreased without ZFP57.

$NKX2.5^+$ Cells Exhibited Proliferation Defect. We also found the fraction of $NKX2.5^+$ cells that were EdU^+ was reduced in the heart of $^{-/-}mz$ (M^-Z^-) E13.5 embryos compared with $^{-/+}$ (M^-Z^+) E13.5 embryos (*SI Appendix*, Fig. S10*A*). When quantified, it was significantly reduced in the whole heart (*SI Appendix*, Fig. S10*B*). If measured separately, it was significantly reduced in the ventricle and ventricular septum but not in the atria (*SI Appendix*, Fig. S10*C*). These results suggest that $NKX2.5^+$ cells exhibited reduced proliferation without ZFP57.

c-KIT^+ Cells Displayed Increased Proliferation. Interestingly, we found c-KIT^+ cells had increased proliferation in the heart of $^{-/-}mz$ (M^-Z^-) E13.5 embryos compared with $^{-/+}$ (M^-Z^+) E13.5 embryos (*SI Appendix*, Fig. S11*A*). When quantified in the whole heart, the fraction of c-KIT^+ cells that were EdU^+ was significantly increased in $^{-/-}mz$ (M^-Z^-) E13.5 embryos in comparison with $^{-/+}$ (M^-Z^+) E13.5 embryos (*SI Appendix*, Fig. S11*B*). When quantified separately, it was significantly increased in the ventricle and ventricular septum but not in the atria (*SI Appendix*, Fig. S11*C*). These results suggest that c-KIT^+ cells exhibited increased cell proliferation without ZFP57.

Discussion

Maternal and zygotic *Zfp57* play redundant roles in the survival of mouse embryos (13). In this study, we found that *Zfp57* mutants exhibited multiple cardiac defects, with the maternal-zygotic mutant displaying higher penetrance and more severe phenotypes than the zygotic mutant. Indeed, we found expression of some key players in cardiac development such as *Hey2*, *Nkx2.5*, and *Gata4* was only severely down-regulated in the *Zfp57* maternal-zygotic mutant E13.5 embryos, less so in E10.5 embryos, but not in *Zfp57* zygotic mutant or heterozygous embryos with or without maternal *Zfp57* (Fig. 3 and *SI Appendix*, Figs. S5, S6, and S8). These results suggest that maternal *Zfp57*, together with zygotic *Zfp57*, contributes to cardiac development. Maternal and zygotic *Zfp57* play redundant roles in normal cardiac septation and ventricular wall thickness. This serves as an example of maternal function that is involved in mammalian organ development. Surprisingly, zygotic *Zfp57* appears to be necessary and sufficient for *Bmp10* expression and ventricular trabeculation in the embryonic heart (Figs. 1*E* and 3). Therefore, maternal and zygotic *Zfp57* are partially redundant in cardiac development, with maternal *Zfp57* functioning in some but not all processes.

ZFP57 is required for the maintenance of the DNA methylation imprint at a large number of imprinted regions in both mouse and humans (13, 17). Maternal and zygotic *Zfp57* are partially redundant in its maintenance (13). DNA methylation at the imprinting control regions is essential for proper expression of the imprinted genes (14, 16, 42). Previously, we hypothesized that maternal *Zfp57* may exert its effect on the late stage of mouse embryonic development through its roles in the maintenance of the DNA methylation imprint in early mouse embryos (43). In this case, maternal *Zfp57*, together with zygotic *Zfp57*, maintains the DNA methylation imprint at some target imprinted regions that control expression of certain imprinted genes required for cardiac development in mouse embryos. For example, expression of the imprinted *Dlk1* gene is dependent on DNA methylation at the IG-DMR, the imprinting control region of the *Dlk1-Dio3* imprinted region (22, 44). In this study, we found both the DNA methylation imprint at the IG-DMR and expression of *Dlk1* were lost in the embryonic heart without ZFP57 (Fig. 2 *B* and *C* and *SI Appendix*, Fig. S4 *A* and *B*). Furthermore, we found that loss of ZFP57 causes cardiac defects that are reminiscent of various knockout mice in the NOTCH signaling pathway (Fig. 6). Further analysis revealed that NOTCH1 activation was inhibited in the heart of *Zfp57* mutant embryos. Expression of *Hey2*, *Nkx2.5*, and *Bmp10*, three target genes of NOTCH1, was down-regulated in the heart without ZFP57 confirming that NOTCH signaling was attenuated in the heart of *Zfp57* mutants. Together these results support our hypothesis that maternal and zygotic *Zfp57* influence cardiac development through regulating DNA methylation imprint and expression of the imprinted genes that function in NOTCH signaling.

The imprinted *Dlk1* gene is highly expressed during embryogenesis (45–49). It is also called Pref-1, a factor involved in adipogenesis (20, 21, 50). Some previous studies had implicated DLK1 and its homologs as positive regulators in LIN-12/NOTCH signaling (25, 51, 52), whereas other studies had shown the opposite or no effect of DLK1 on NOTCH signaling (26, 27, 50, 53–56). These seemingly contradictory results could be due to different experimental systems used in different studies. Another possible explanation for these discrepancies could be caused by the complex expression pattern and structure of the imprinted

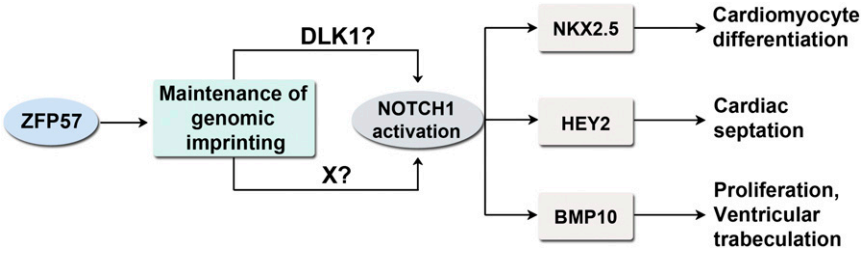

Fig. 6. A schematic model is proposed for the probable molecular mechanisms of ZFP57 in Notch signaling and cardiac development. ZFP57 maintains genomic imprinting and it is required for the proper expression of its target imprinted genes including *Dlk1*. DLK1 and/or other target gene product of ZFP57 (indicated by factor X here) may activate NOTCH1 to generate N1ICD that can stimulate transcription of the NOTCH1 target genes in the embryonic heart. NOTCH1 activation could be either DLK1 dependent or DLK1 independent. NKX2.5, HEY2, and BMP10 are three downstream targets of NOTCH1 that control cardiomyocyte differentiation, cardiac septation, proliferation, and ventricular trabeculation, respectively.

Dlk1 gene (47, 49). It is reported that there are various isoforms of *Dlk1* transcripts that produce membrane-bound or secreted DLK1 proteins (13, 24, 49, 53, 57–59). The membrane-bound form of DLK1 can also be cleaved to generate soluble peptides (58). These different isoforms of DLK1 proteins could exhibit opposite effects in cell signaling and development (45, 55, 60, 61). Therefore, DLK1 may act as a positive or negative regulator of NOTCH signaling under different conditions. The cumulative effect of various DLK1 proteins may also result in no effect on NOTCH signaling under certain circumstances.

Most N1ICD$^+$ cells were DLK1$^+$ in the heart of heterozygous, $^{-/+}$ (M^-Z^+), embryos, whereas the N1ICD$^+$DLK1$^+$ cells were almost absent in the maternal-zygotic mutant, $^{-/-}$*mz* (M^-Z^-), embryos (Fig. 2 *F* and *G*). We propose here that DLK1 may be involved in NOTCH1 activation in cardiac development (Fig. 6). Intriguingly, a small portion of N1ICD$^+$ cells were DLK1$^-$, indicative of DLK1-independent NOTCH1 activation, that remained constant in the heart of heterozygous, $^{-/+}$ (M^-Z^+), or maternal-zygotic mutant, $^{-/-}$*mz* (M^-Z^-), embryos (Fig. 2 *F* and *G*). These results suggest that DLK1 probably promotes N1ICD generation and DLK1-mediated NOTCH1 activation may account for most N1ICD in the heart of heterozygous $^{-/+}$ (M^-Z^+) embryos. This may be one of the first instances implicating DLK1 as a positive regulator in NOTCH signaling in mammalian heart development.

Intriguingly, DLK1 and N1ICD were present in the same cells in the embryonic heart. We hypothesize that DLK1 may act as a cofactor such as a coreceptor, rather than a noncanonical ligand, for NOTCH1 and other NOTCH receptors. Alternatively, DLK1 may activate NOTCH signaling by recycling and/or presenting NOTCH receptor proteins for activation by canonical DSL ligands. It is also possible that DLK1 functions as a ligand for NOTCH1 and other NOTCH receptors within the same cells to activate NOTCH receptors through an autocrine mechanism (29). These hypotheses need to be tested in the future by investigating the specific interactions of DLK1 and NOTCH receptors.

It is also plausible that ZFP57 activates NOTCH1 via a DLK1-independent pathway (via factor X in Fig. 6), with DLK1 being just a bystander in the NOTCH1 receptor activation process. Based on current data, we could not distinguish these possibilities. However, there have been a number of papers suggesting a probable role of DLK1 in LIN-12/NOTCH signaling regardless of whether it is a positive or negative regulator (25–27, 51, 52, 56). Therefore, we favor our current model that DLK1, probably together with other target genes of ZFP57 (e.g., factor X in Fig. 6), is involved in NOTCH1 activation.

Loss of ZFP57 caused accumulation of c-KIT$^+$ cells and decrease of NKX2.5$^+$ or GATA4$^+$ cells in the heart. Although we need to use antibodies against some markers of cardiomyocytes for coimmunostaining to confirm these cell identities, we think NKX2.5$^+$ or GATA4$^+$ cells are likely immature committed cardiomyocytes that are decreased in the embryonic heart of *Zfp57* mutant embryos. These results implicating cell differentiation defects are consistent with attenuation of NOTCH signaling in the heart without ZFP57. Indeed, LIN-12/NOTCH signaling is essential for cell-fate specification (8). This differentiation block, together with cell proliferation defect, may result in most cardiac defects observed in *Zfp57* mutants (Fig. 6).

Both mouse and human ZFP57 proteins maintain genomic imprinting (13, 17). Interestingly, some human patients with *ZFP57* mutations exhibited partially penetrant ASD, VSD, and tetralogy of Fallot (TOF) (17), resembling those present in the *Zfp57* zygotic mutant (Fig. 1). Based on this observation, we hypothesize that human *ZFP57* mutations may also compromise NOTCH signaling.

Materials and Methods

Mouse Breeding and Timed Pregnancy Mating. The animal protocol was approved by the Institutional Animal Care and Use Committee (IACUC) of the Icahn School of Medicine at Mount Sinai. All mouse strains were on a mixed genetic background of 129Sv/Ev and Black Swiss origins. *Zfp57* mutant mice containing the deleted null allele of *Zfp57* were used here for timed pregnancy mating (13). Noon of the day when vaginal plug was found was counted as the half-day pregnancy (E0.5). *Zfp57* zygotic mutant, $^{-/-}$*z* (M^+Z^-), embryos lacking just the zygotic *Zfp57* and heterozygous, $^{+/-}$ (M^+Z^+), embryos with both maternal and zygotic *Zfp57* were generated from the cross between heterozygous ($^{+/-}$) female mice and homozygous ($^{-/-}$) male mice or from the cross between heterozygous ($^{+/-}$) female mice and heterozygous ($^{+/-}$) male mice (*SI Appendix*, Fig. S1). Similarly, *Zfp57* maternal-zygotic mutant, $^{-/-}$*mz* (M^-Z^-), embryos without maternal or zygotic *Zfp57*, and heterozygous, $^{-/+}$ (M^-Z^+), embryos lacking maternal *Zfp57*, were generated from the cross between homozygous ($^{-/-}$) female mice and heterozygous ($^{+/-}$) male mice (*SI Appendix*, Fig. S1).

Histological Analysis and Quantification. Embryos or heart samples isolated from pregnant mice were fixed in 4% (wt/vol) of paraformaldehyde (PFA) solution overnight and embedded in paraffin. Transverse serial sections of 8 μm in thickness were stained with hematoxalin and eosin (H&E). Ventricular wall (vw) thickness and trabecular area were measured by ImageJ software on comparable sections through the atrioventricular canal region for five separate embryos for each genotype. For vw, four measurements were made in the selected areas of the left and right ventricles of each embryo. Total average trabecular area was quantified in the left and right ventricles of each embryo.

RNA in Situ Hybridization with Digoxigenin Labeling. Sense and antisense probes were made of a DIG RNA labeling kit (Roche). Embryos fixed in 4% (wt/vol) of PFA solution for 24 h were dehydrated in either 30% (wt/vol) or 2 M of sucrose solution before being embedded in OCT compound (Sakura). Transverse serial cryosections of 10 μm in thickness obtained from these embryos were incubated with sense or antisense digoxigenin-labeled RNA probe at 65 °C overnight. Alkaline phosphatase (AP) substrate was added to the sections for detection after incubation with AP-coupled antidigoxigenin antibody.

Immunohistochemical Analysis and Quantification. Samples were fixed in 4% (wt/vol) of PFA solution for 4 h to overnight at 4 °C and embedded in paraffin or OCT. Transverse serial sections of 8 μm in thickness were obtained for immunostaining. Sodium citrate antigen retrieval was applied to paraffin sections. For NOTCH1 or N1ICD immunostaining, paraffin sections or cryosections were blocked with 5% (vol/vol) goat serum for 1 h at room temperature (RT) followed by incubation with rabbit monoclonal antibodies against NOTCH1 (1:100, Cell Signaling 3608) or N1ICD (1:100, Cell Signaling 4147) at 4 °C overnight. After incubation with the primary antibodies, these sections were incubated with biotinylated goat anti-rabbit IgG (1:300, Vector BA1000) secondary antibodies for 1 h at RT followed by the signal amplification procedure with TSA Plus Cy3 System (Perkin-Elmer) that was performed according to the manufacturer's suggested protocol. For c-KIT, NKX2.5, or GATA4 immunostaining, cryosections were blocked with 5% (vol/vol) donkey serum for 1 h at RT followed by incubation with goat anti–c-KIT (1:300, R&D AF1356), goat anti-NKX2.5 (1:300, Santa Cruz SC8697), or goat anti-GATA4 (1:600, Santa Cruz SC1237) antibodies. After incubation with the primary antibodies, these sections were incubated with biotinylated donkey anti-goat IgG (1:300, Millipore AP180B) secondary antibodies for 1 h at RT followed by the signal amplification procedure with TSA Plus Cy3 System. For cleaved Caspase-3 immunostaining, paraffin sections were blocked with 5% (vol/vol) of goat serum for 1 h at RT followed by incubation with rabbit anti-cleaved Caspase-3 (1:500, Cell Signaling 9664) antibody at 4 °C overnight. After incubation with the primary antibodies, these sections were incubated with biotinylated goat anti-rabbit IgG (1:300, Vector BA1000) secondary antibodies for 1 h at RT followed by signal amplification with TSA Plus Cy3 System. For DLK1 immunostaining, cryosections were incubated with rat anti-DLK1 antibody (Enzo Life Sciences PF105B) at 4 °C overnight and then stained with FITC-labeled goat anti-rat IgG (1:300, Southern Biotech 3030-02) secondary antibodies for 1 h at RT. All stained sections were imaged under a Axioplan2IE microscope with Apotome (Zeiss). Immunofluorescent cells were counted on comparable sections with ImageJ software for at least three separate embryos for each genotype.

EdU Incorporation Assay. Pregnant female mice were injected with 25 μg of EdU (Molecular Probes) per gram of body weight 1 h before embryos were collected for fixation. The embryos were fixed in 4% (wt/vol) of PFA for 4 h at 4 °C and embedded in OCT. Transverse serial sections of 8 μm in thickness obtained from these embryos were stained with Click-iT Imaging Kit (Molecular Probes).

Statistical Analysis. Statistical analyses were performed using Microsoft Excel. All results are reported as mean ± SEM of at least three independent

samples. Student's *t* test was used for statistical comparisons between two groups of data. The results with $^{**}P < 0.01$ and $^{*}P < 0.05$ were considered statistically significant in Student's *t* test. One-way analysis of variance (ANOVA) was performed for statistical comparisons of more than two groups of data, followed by the post hoc independent sample *t* test with Bonferroni correction. The results with $^{*}P < 0.05$ were considered statistically significant in ANOVA.

ACKNOWLEDGMENTS. The authors thank Drs. James Bieker, Bruce Gelb, and Paul Wassarman of Icahn School of Medicine at Mount Sinai for their critical reading of the manuscript. Microscopy was performed at the Microscopy CORE facility located at the Icahn School of Medicine at Mount Sinai. This work was supported by National Institutes of Health (NIH) Grant GM093335, NYSTEM Contract C026434, and American Heart Association Grant 09SDG2400151 (to X.L.). Y.S. and D.E.C. were partly supported by NIH T32 Cancer Biology or Developmental Biology Training Grants, respectively.

1. Zaidi S, et al. (2013) De novo mutations in histone-modifying genes in congenital heart disease. *Nature* 498(7453):220–223.
2. Lin CJ, Lin CY, Chen CH, Zhou B, Chang CP (2012) Partitioning the heart: Mechanisms of cardiac septation and valve development. *Development* 139(18):3277–3299.
3. Bruneau BG (2008) The developmental genetics of congenital heart disease. *Nature* 451(7181):943–948.
4. Fahed AC, Gelb BD, Seidman JG, Seidman CE (2013) Genetics of congenital heart disease: The glass half empty. *Circ Res* 112(4):707–720.
5. Greenwald I, Kovall R (2013) Notch signaling: Genetics and structure. *WormBook* 1–28.
6. Kopan R (2012) Notch signaling. *Cold Spring Harb Perspect Biol* 4(10).
7. Artavanis-Tsakonas S, Muskavitch MA (2010) Notch: The past, the present, and the future. *Curr Top Dev Biol* 92:1–29.
8. Greenwald I (1998) LIN-12/Notch signaling: Lessons from worms and flies. *Genes Dev* 12(12):1751–1762.
9. MacGrogan D, Nus M, de la Pompa JL (2010) Notch signaling in cardiac development and disease. *Curr Top Dev Biol* 92:333–365.
10. Jain R, Rentschler S, Epstein JA (2010) Notch and cardiac outflow tract development. *Ann N Y Acad Sci* 1188:184–190.
11. Gridley T (2010) Notch signaling in the vasculature. *Curr Top Dev Biol* 92:277–309.
12. Boni A, et al. (2008) Notch1 regulates the fate of cardiac progenitor cells. *Proc Natl Acad Sci USA* 105(40):15529–15534.
13. Li X, et al. (2008) A maternal-zygotic effect gene, *Zfp57*, maintains both maternal and paternal imprints. *Dev Cell* 15(4):547–557.
14. Bartolomei MS, Ferguson-Smith AC (2011) Mammalian genomic imprinting. *Cold Spring Harb Perspect Biol* 3(7).
15. Li X (2013) Genomic imprinting is a parental effect established in mammalian germ cells. *Curr Top Dev Biol* 102:35–59.
16. Barlow DP (2011) Genomic imprinting: A mammalian epigenetic discovery model. *Annu Rev Genet* 45:379–403.
17. Mackay DJ, et al. (2008) Hypomethylation of multiple imprinted loci in individuals with transient neonatal diabetes is associated with mutations in ZFP57. *Nat Genet* 40(8):949–951.
18. Conway SJ, Kruzynska-Frejtag A, Kneer PL, Machnicki M, Koushik SV (2003) What cardiovascular defect does my prenatal mouse mutant have, and why? *Genesis* 35(1): 1–21.
19. Chen H, et al. (2004) BMP10 is essential for maintaining cardiac growth during murine cardiogenesis. *Development* 131(9):2219–2231.
20. Laborda J, Sausville EA, Hoffman T, Notario V (1993) dlk, a putative mammalian homeotic gene differentially expressed in small cell lung carcinoma and neuroendocrine tumor cell line. *J Biol Chem* 268(6):3817–3820.
21. Smas CM, Sul HS (1993) Pref-1, a protein containing EGF-like repeats, inhibits adipocyte differentiation. *Cell* 73(4):725–734.
22. Schmidt JV, Matteson PG, Jones BK, Guan XJ, Tilghman SM (2000) The *Dlk1* and *Gtl2* genes are linked and reciprocally imprinted. *Genes Dev* 14(16):1997–2002.
23. Takada S, et al. (2000) Delta-like and *gtl2* are reciprocally expressed, differentially methylated linked imprinted genes on mouse chromosome 12. *Curr Biol* 10(18): 1135–1138.
24. Kopan R, Ilagan MX (2009) The canonical Notch signaling pathway: Unfolding the activation mechanism. *Cell* 137(2):216–233.
25. Komatsu H, et al. (2008) OSM-11 facilitates LIN-12 Notch signaling during Caenorhabditis elegans vulval development. *PLoS Biol* 6(8):e196.
26. Baladrón V, et al. (2005) dlk acts as a negative regulator of Notch1 activation through interactions with specific EGF-like repeats. *Exp Cell Res* 303(2):343–359.
27. Bray SJ, Takada S, Harrison E, Shen SC, Ferguson-Smith AC (2008) The atypical mammalian ligand Delta-like homologue 1 (*Dlk1*) can regulate Notch signalling in Drosophila. *BMC Dev Biol* 8:11.
28. Fortini ME (2009) Notch signaling: The core pathway and its posttranslational regulation. *Dev Cell* 16(5):633–647.
29. D'Souza B, Meloty-Kapella L, Weinmaster G (2010) Canonical and non-canonical Notch ligands. *Curr Top Dev Biol* 92:73–129.
30. Struhl G, Greenwald I (1999) Presenilin is required for activity and nuclear access of Notch in Drosophila. *Nature* 398(6727):522–525.
31. Fischer A, Schumacher N, Maier M, Sendtner M, Gessler M (2004) The Notch target genes Hey1 and Hey2 are required for embryonic vascular development. *Genes Dev* 18(8):901–911.
32. Donovan J, Kordylewska A, Jan YN, Utset MF (2002) Tetralogy of fallot and other congenital heart defects in *Hey2* mutant mice. *Curr Biol* 12(18):1605–1610.
33. Gessler M, et al. (2002) Mouse gridlock: No aortic coarctation or deficiency, but fatal cardiac defects in *Hey2 -/-* mice. *Curr Biol* 12(18):1601–1604.
34. Sakata Y, et al. (2002) Ventricular septal defect and cardiomyopathy in mice lacking the transcription factor CHF1/Hey2. *Proc Natl Acad Sci USA* 99(25):16197–16202.
35. McCulley DJ, Black BL (2012) Transcription factor pathways and congenital heart disease. *Curr Top Dev Biol* 100:253–277.
36. Grego-Bessa J, et al. (2007) Notch signaling is essential for ventricular chamber development. *Dev Cell* 12(3):415–429.
37. Moens CB, Stanton BR, Parada LF, Rossant J (1993) Defects in heart and lung development in compound heterozygotes for two different targeted mutations at the *N-myc* locus. *Development* 119(2):485–499.
38. Charron J, et al. (1992) Embryonic lethality in mice homozygous for a targeted disruption of the N-myc gene. *Genes Dev* 6(12A):2248–2257.
39. Muller-Sieburg CE, Sieburg HB, Bernitz JM, Cattarossi G (2012) Stem cell heterogeneity: Implications for aging and regenerative medicine. *Blood* 119(17):3900–3907.
40. Boisset JC, et al. (2010) In vivo imaging of haematopoietic cells emerging from the mouse aortic endothelium. *Nature* 464(7285):116–120.
41. Scott IC (2012) Life before Nkx2.5: Cardiovascular progenitor cells: Embryonic origins and development. *Curr Top Dev Biol* 100:1–31.
42. Li E, Beard C, Jaenisch R (1993) Role for DNA methylation in genomic imprinting. *Nature* 366(6453):362–365.
43. Li X (2010) Extending the maternal-zygotic effect with genomic imprinting. *Mol Hum Reprod* 16(9):695–703.
44. Lin SP, et al. (2003) Asymmetric regulation of imprinting on the maternal and paternal chromosomes at the *Dlk1-Gtl2* imprinted cluster on mouse chromosome 12. *Nat Genet* 35(1):97–102.
45. Falix FA, Aronson DC, Lamers WH, Gaemers IC (2012) Possible roles of DLK1 in the Notch pathway during development and disease. *Biochim Biophys Acta* 1822(6): 988–995.
46. Appelbe OK, Yevtodiyenko A, Muniz-Talavera H, Schmidt JV (2013) Conditional deletions refine the embryonic requirement for *Dlk1*. *Mech Dev* 130(2-3):143–159.
47. Rogers ED, Ramalie JR, McMurray EN, Schmidt JV (2012) Localizing transcriptional regulatory elements at the mouse *Dlk1* locus. *PLoS ONE* 7(5):e36483.
48. da Rocha ST, et al. (2007) Restricted co-expression of *Dlk1* and the reciprocally imprinted non-coding RNA, *Gtl2*: implications for cis-acting control. *Dev Biol* 306(2): 810–823.
49. Miller AJ, Cole SE (2014) Multiple *Dlk1* splice variants are expressed during early mouse embryogenesis. *Int J Dev Biol* 58(1):65–70.
50. Sul HS (2009) Minireview: Pref-1: Role in adipogenesis and mesenchymal cell fate. *Mol Endocrinol* 23(11):1717–1725.
51. Singh K, et al. (2011) *C. elegans* Notch signaling regulates adult chemosensory response and larval molting quiescence. *Curr Biol* 21(10):825–834.
52. Li L, et al. (2014) DLK1 promotes lung cancer cell invasion through upregulation of MMP9 expression depending on Notch signaling. *PLoS ONE* 9(3):e91509.
53. Ferrón SR, et al. (2011) Postnatal loss of *Dlk1* imprinting in stem cells and niche astrocytes regulates neurogenesis. *Nature* 475(7356):381–385.
54. Müller D, et al. (2014) *Dlk1* promotes a fast motor neuron biophysical signature required for peak force execution. *Science* 343(6176):1264–1266.
55. Andersen DC, et al. (2013) Dual role of delta-like 1 homolog (DLK1) in skeletal muscle development and adult muscle regeneration. *Development* 140(18):3743–3753.
56. Schober A, et al. (2014) MicroRNA-126-5p promotes endothelial proliferation and limits atherosclerosis by suppressing *Dlk1*. *Nat Med* 20(4):368–376.
57. Smas CM, Chen L, Zhao L, Latasa MJ, Sul HS (1999) Transcriptional repression of pref-1 by glucocorticoids promotes 3T3-L1 adipocyte differentiation. *J Biol Chem* 274(18): 12632–12641.
58. Smas CM, Chen L, Sul HS (1997) Cleavage of membrane-associated pref-1 generates a soluble inhibitor of adipocyte differentiation. *Mol Cell Biol* 17(2):977–988.
59. Garcés C, Ruiz-Hidalgo MJ, Bonvini E, Goldstein J, Laborda J (1999) Adipocyte differentiation is modulated by secreted delta-like (dlk) variants and requires the expression of membrane-associated dlk. *Differentiation* 64(2):103–114.
60. Shin S, Suh Y, Zerby HN, Lee K (2014) Membrane-bound delta-like 1 homolog (*Dlk1*) promotes while soluble Dlk1 inhibits myogenesis in C2C12 cells. *FEBS Lett* 588(7): 1100–1108.
61. Traustadottir GA, Kosmina R, Sheikh SP, Jensen CH, Andersen DC (2013) Preadipocytes proliferate and differentiate under the guidance of Delta-like 1 homolog (DLK1). *Adipocyte* 2(4):272–275.